


T.V. Shulyatnikova\*, V.O. Tumanskiy, L.M. Tumanska 

## PATHOMORPHOLOGY OF SEVERE GRADE 3-4 HEPATIC ENCEPHALOPATHY IN DECOMPENSATED CIRRHOSIS PATIENTS WITH ACUTE-ON-CHRONIC LIVER FAILURE

Zaporizhzhia State Medical and Pharmaceutical University  
Maiakovskiy av., 26, Zaporizhzhia, 69035, Ukraine  
Запорізький державний медико-фармацевтичний університет  
пр. Маяковського, 26, Запоріжжя, 69035, Україна  
\*e-mail: shulyatnikova.tv@gmail.com

*Цитування: Медичні перспективи. 2024. Т. 29, № 2. С. 62-71*

*Cited: Medicni perspektivi. 2024;29(2):62-71*

**Key words:** hepatic encephalopathy, liver cirrhosis, neuropathology, immunohistochemistry, ammonia, Alzheimer type 2 astrocytes, amoeboid microglia, amyloid bodies

**Ключові слова:** печінкова енцефалопатія, цироз печінки, патоморфологія, імуногістохімія, аміак, астроцити Альцгеймера 2 типу, амебоїдна мікроглія, амілоїдні тільця

**Abstract.** Pathomorphology of severe Grade 3-4 hepatic encephalopathy in decompensated cirrhosis patients with acute-on-chronic liver failure. Shulyatnikova T.V., Tumanskiy V.O., Tumanska L.M. The study was aimed to determine of the most significant pathomorphological signs of severe hepatic encephalopathy (HE) in deceased cirrhotic patients with acute-on-chronic liver failure (ACLF) syndrome based on changes of the glioneuronal complex and the level of tissue ammonia. Using pathohistological, histochemical, and immunohistochemical methods, the cerebral cortex, thalamus, striatum, and cerebellum of 21 deceased patients with acutely decompensated liver cirrhosis with ACLF syndrome and HE Grade 3-4 were examined in comparison with control group, which included 30 deceased patients from acute cardiovascular failure. The study revealed that during HE Grade 3-4 as a component of ACLF, in all studied brain regions, there was a reliably ( $p < 0.05$ ) higher histochemical level of tissue ammonia (up to 500%), increased numbers (up to 215.69%) of apoptotic neurons (according to caspase-3), reduced (up to 119.60%) level of synaptophysin, increased expression of glutamine synthetase (up to 253.02%) and aquaporin-4 (up to 481.81%) associated by reduced (up to 296.81%) expression of glial fibrillary acidic protein in astrocytes, increased (up to 11-fold) numbers of Alzheimer type 2-astrocytes, expansion of perivascular and pericellular «edematous» spaces (up to 890.81%), increased numbers of amyloid bodies (up to 5-fold), increased area of immunopositive material of CD68+ microglia (up to 114.78%) with an increase (up to 71.91%) in the proportion of CD68+ amoeboid microglia. The above-mentioned changes confirm that the loss of consciousness and other psychoneurological manifestations of severe HE Grade 3-4 are due to compound ammonia-associated changes in the components of the glioneuronal complex, namely: adaptive remodeling and dystrophic changes in astrocytes, reduced synaptic transmission and apoptotic neuronal death, reactive changes in microglia with a small proportion of microglia involved in phagocytosis, cytotoxic brain edema and dysfunction of the lymphatic system.

**Реферат.** Патоморфологія 3-4 ступенів тяжкості печінкової енцефалопатії у хворих на декомпенсований цироз печінки з синдромом гострої на тлі хронічної печінкової недостатності. Шулятнікова Т.В., Туманський В.О., Туманська Л.М. Дослідження присвячене визначенню найбільш суттєвих патоморфологічних ознак тяжкої печінкової енцефалопатії (ПЕ) у померлих хворих на цироз печінки з синдромом гострої на тлі хронічної печінкової недостатності (ГХПечН) на підставі змін гліонейронального комплексу та рівня тканинного аміаку. За допомогою патогістологічних, гістохімічних, імуногістохімічних методів досліджено кору великих півкуль головного мозку (ГМ), таламус, смугасте тіло, мозочок 21 померлого хворого на гостро декомпенсований цироз печінки із синдромом ГХПечН та ПЕ Grade 3-4 в порівнянні з групою контролю, що включила з 30 померлих від гострої серцево-судинної недостатності пацієнтів без ПЕ. Результати дослідження показали, що при ПЕ 3-4 ступенів тяжкості в складі синдрому ГХПечН з у всіх досліджених відділах ГМ виявляється достовірно ( $p < 0,05$ ) і значно вищий (до 500%) рівень тканинного аміаку, підвищена кількість (до 215,69%) апоптотичних нейронів (за каспазою-3) та знижений (до 119,60%) рівень експресії синаптофізину, підвищений (до 253,02%) рівень експресії глутамінсинтетази і аквапорину-4 (до 481,81%) та знижений (до 296,81%) рівень експресії гліофібрилярного білку в астроцитах, підвищена (до 11 разів) кількість астроцитів Альцгеймера 2 типу, значне (до 890,81%) розширення периваскулярних і перицелюлярних «набрякових» просторів, підвищена (до 5 разів)

кількість амілоїдних тілець, підвищена (до 114,78%) площа експресії CD68+ мікрогліоцитів та збільшена (до 71,91%) частка CD68+ амебоїдних мікрогліоцитів. Отримані дані свідчать про те, що зниження свідомості та інші психоневрологічні прояви тяжкої ПЕ 3-4 ступенів тяжкості зумовлені аміак-асоційованими морфофункціональними змінами гліонейронального комплексу, а саме: адаптивним ремоделюванням та дистрофічними змінами астроцитів, зниженням синаптичної передачі та апоптозом нейронів, реактивними змінами мікроглії з незначним зростанням частки фагоцитуючих мікрогліоцитів, а також цитотоксичним набряком ГМ та дисфункцією глімфатичної системи.

Hepatic encephalopathy (HE) in patients with liver cirrhosis (LC) is believed to be conditioned by ammonia-induced astroglipathy [1, 2, 3], which, according to the results of our recent studies [4], is associated with an increased optical density of tissue ammonia precipitates, altered expression of key astroglial proteins (GFAP, GS, and AQP4) and the appearance of numerous Alzheimer type 2 astrocytes (AA2) in the thalamus, striatum, cerebellum and cerebral cortex. In patients with acute decompensation of LC (acute development of refractory ascites and/or gastrointestinal bleeding, systemic inflammation, jaundice), severe HE occurs as a component of the most dangerous syndrome during LC – acute-on-chronic liver failure (ACLF) [5], when the above symptoms of acute decompensation of LC are aggravated by signs of organ dysfunction/failure (liver and/or kidney, brain, lung, circulatory), which is associated with an extremely high rate of a short-term mortality (< 28 days after hospital admission) [6]. According to CLIF-C OF scale assessment of ACLF [7], decreased consciousness of cirrhotic patients up to deep stupor (12-11 points of Glasgow coma scale [GCS]) is referred as HE Grade 3, and comatose state ( $\leq 8$  points according to GCS) – as HE Grade 4. Despite the fact that severe Grade 3-4 HE significantly increases cirrhotic patients mortality rates and affects thanatogenesis, its pathomorphological characteristics is lacking and was only partially described by selected studies [1, 8]. Considering the above, the current study was aimed to determine the most important pathomorphological signs of severe Grade 3-4 HE in deceased cirrhotic patients with ACLF based on the glioneuronal complex changes and the level of brain tissue ammonia.

#### MATERIALS AND METHODS OF RESEARCH

The study was performed on autopsy material of 21 deceased patients with acutely decompensated non-alcoholic LC of class C according to Child-Pugh scale [9], aged 55-83 y.o. (mean age  $60.00 \pm 7.07$  y.o.) associated with HE Grade 3 (n=14) and Grade 4 (n=7). According to the CLIF-C OF scale, these patients additionally manifested intravital signs of acute liver and/or kidney, circulatory dysfunction/failure (based on the serum bilirubin, creatinine and mean arterial pressure, respectively), as well as laboratory signs of systemic inflammation (leukocytosis, increased ESR and leukocyte intoxication index),

which corresponded to criteria for ACLF according to EASL-CLIF (Table) [7].

The conditional control group included patients who died from acute cardiovascular failure without toxic-metabolic pathologies and signs of encephalopathy (n=30).

The study meets the requirements stated in the Declaration of Helsinki «Ethical principles of medical research involving human subjects» of the World Medical Association, the «General Declaration on Bioethics and Human Rights (UNESCO)», the Order of the Ministry of Health of Ukraine «On Approval of the Procedure for Conducting Clinical Trials of Medicinal Products and examination of materials of clinical trials and a standard regulation on ethics commissions» No. 690, 09/23/2009, and was approved by the local Bioethics committee of Zaporizhzhia State Medical and Pharmaceutical University (protocol No. 13, March 15, 2024). Pathomorphological studies of the brain were performed within the standard list of brain regions necessary for diagnosing the causes of death.

Cortical samples from the frontal, parietal, temporal, and occipital lobes of the cerebral large hemispheres, thalamus, striatum, and cerebellum were fixed in 10% buffered formalin and embedded in paraffin blocks. Serial 4  $\mu\text{m}$  sections for microscopic analysis (hematoxylin and eosin staining), histochemical (HC) and immunohistochemical (IHC) studies were produced by the precession rotary microtome HM3600 («MICROM Laborgerate GmbH» – Germany). Ammonia determination in paraffin brain sections was performed by HC method using Nessler's reagent according to V. Gutiérrez-de-Juan et al. [10]. IHC studies were run in paraffin sections according to the manufacturer's instructions using the UltraVision Quanto HRP + DAB System visualization system (Thermo Scientific, USA). The level of neuronal apoptotic changes was detected using Mo a-Hu Caspase 3 (Casp3) (CPP32) Ab-3 (*Clone 3CSP03*, Thermo Scientific Inc., USA); synaptic vesicles quantities in presynaptic terminals were identified by Mo anti-synaptophysin (Syn) Ab (*Clone SY38*, Thermo Scientific Inc., USA); to identify astrocytic changes were used Mo anti-GFAP Ab (*Clone ASTRO6*, Thermo Scientific Inc., USA), Rb polyclonal anti-GS Ab (Thermo Scientific Inc., USA) and Rb polyclonal anti-AQP4 Ab (Thermo Scientific Inc., USA); microglia and amoeboid microgliocytes were identified by Mo a-Hu CD68 Ab (*clone PG-M1*, Dako, Denmark).

**Distribution of ACLF signs in deceased patients  
with acutely decompensated LC according to CLIF-C OF scale [7]**

No.	Organ dysfunction/failure				Precipitating/pre-existing factors					
	brain (he)	liver	kidney	C	P	SAP	SI	A	GIB	J
1	Grade 3	-	-	F	+	-	+	Ao	-	Gd
2	Grade 3	D	-	D	+	-	+	Gd	+	Ao
3	Grade 3	-	-	D	-	+	+	Gd	+	Gd
4	Grade 3	D	D	F	+	-	+	Ao	-	Ao
5	Grade 3	D	D	F	-	-	+	Ao	+	Ao
6	Grade 3	-	D	-	-	-	+	Ao	+	Gd
7	Grade 3	D	D	-	+	-	+	Gd	-	Gd
8	Grade 3	F	D	D	+	-	+	Gd	-	Ao
9	Grade 3	F	-	D	-	-	+	Ao	-	Ao
10	Grade 3	F	-	F	-	-	+	Ao	-	Ao
11	Grade 3	F	D	D	+	-	+	Gd	+	Ao
12	Grade 3	-	D	D	-	-	+	Ao	-	Gd
13	Grade 3	D	D	D	-	+	+	Ao	-	Gd
14	Grade 3	D	-	D	+	-	+	Gd	+	Ao
15	Grade 4	D	F	D	-	+	+	Ao	-	Gd
16	Grade 4	F	D	D	+	+	+	Ao	+	Ao
17	Grade 4	D	-	F	+	-	+	Ao	+	Gd
18	Grade 4	F	F	F	+	-	+	Ao	+	Ao
19	Grade 4	D	D	F	-	+	+	Gd	-	Gd
20	Grade 4	D	F	D	+	-	+	Ao	-	Gd
21	Grade 4	F	D	F	+	+	+	Gd	-	Ao

Notes: C – circulation; P – pneumonia; SAP – spontaneous ascites-peritonitis; SI – systemic inflammation (leukocytosis, increased ESR, leukocyte intoxication index); A – ascites; GIB – gastrointestinal bleeding; J – jaundice; D – acute organ dysfunction; F – acute organ failure; Gd – gradual development; Ao – acute onset.

Morphometric analysis was performed in the microscope Scope A1 «Carl Zeiss» (Germany) with camera Jenoptik Progres Gryphax 60N-C1"1,0x426114 (Germany) using morphometric software. HC ammonia expression and IHC expression of synaptophysin were determined in ImageJ (National Institutes of Health, USA) using automatic mode with standard plug-in color deconvolution «H DAB» in 5 standardized fields of view (SFV) x200 of four mentioned brain regions in each case and were expressed in conventional units of optical density (CUOD). With CUOD values from 0 to 20, ammonia and synaptophysin expression were considered negative («-»); 21-50 – weak («+»); 51-100 – moderate («++»); 101≥ – strong («+++»). Using Videotest-Morphology 5.2.0.158 (LLC «VideoTest»)

software, in 5 SFV x200 of each case, in four brain regions were determined the relative area (Srel.%) of immunopositive material of GFAP, GS, AQP4, and CD68, the percentage of Caspase 3+ neurons (%), and at magnification x400 – percentage of CD68+ amoeboid microgliaocytes (%). In each studied brain region, in 5 SFV x400, the mean area of «empty» (swollen) pericellular and perivascular spaces (PCs+PVs) (μm<sup>2</sup>) as well as the average number of amyloid bodies (AB) was calculated. In 20 SFV of each case, the number of Alzheimer type 2 astrocytes was determined and designed 4 degrees of AA2-astrocytosis: 1-5 AA2 – 0 degree; 6-10 AA2 – I degree (weak AA2-astrocytosis); 11-20 AA2 – II degree (moderate); 21 or more AA2 – III degree (severe) [4].

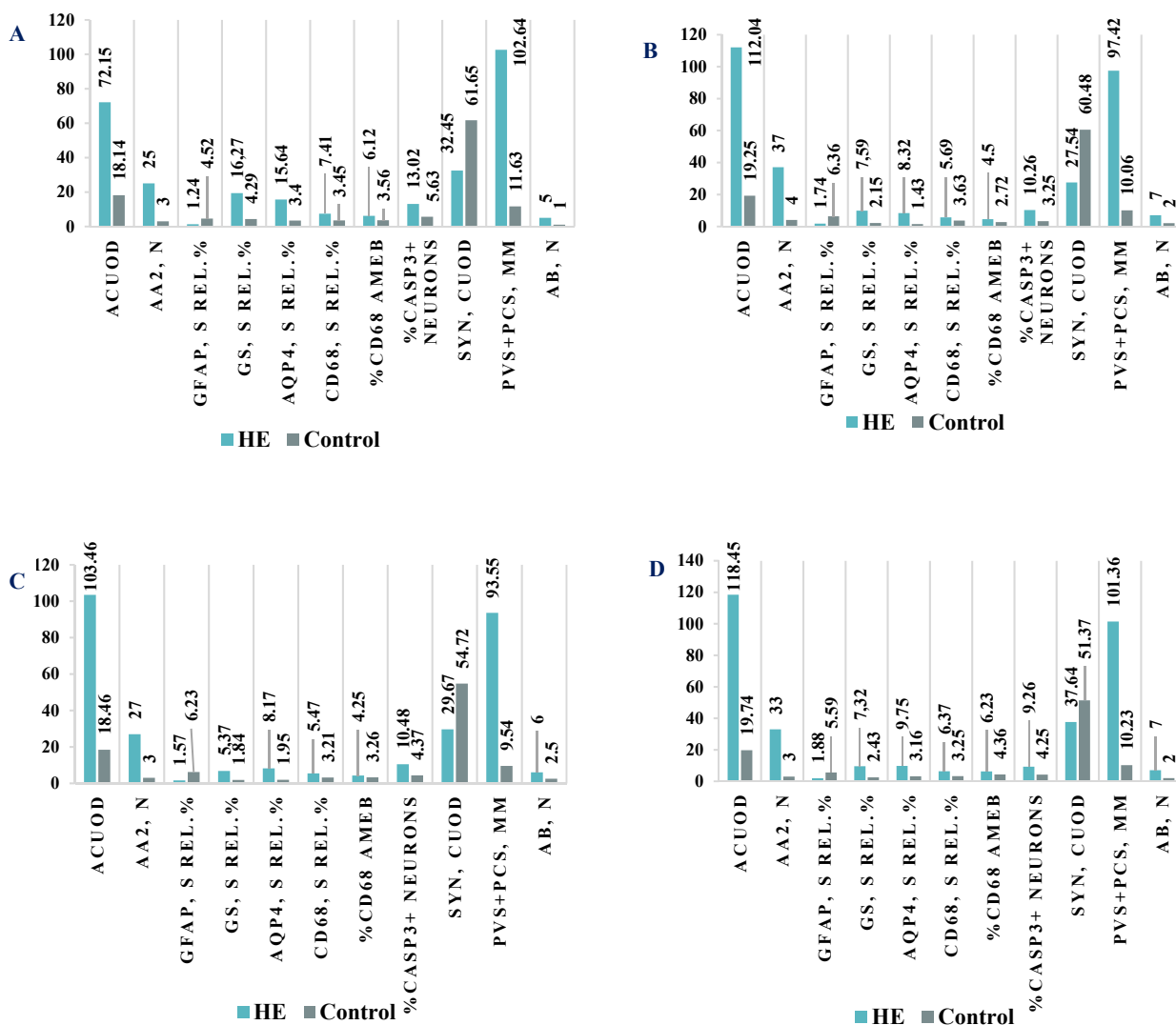


Data were processed using the Statistica® 13.0 package (StatSoft Inc., License No. JPZ804I382130ARCN10-J). Results were represented as median (Me) with range (Q1; Q3). The Mann-Whitney U-test was used to compare two groups, and the Kruskal-Wallis test was used for two or more groups. The results were considered statistically significant at the level of 95% ( $p < 0.05$ ) [11].

**RESULTS AND DISCUSSION**

Considering the results obtained, we can assume that loss of consciousness and other neurological symptoms of HE in ACLF are conditioned by neurotoxic, ammonia-induced significant morpho-functional changes of the glioneuronal complex, which can be determined by pathomorphological examination of cerebral cortex, thalamus, striatum and cerebellum. In

the named brain regions of deceased patients with ACLF and HE Grade 3-4, moderate and strong granular expression of ammonia precipitates reliably ( $p < 0.05$ ) and significantly exceeded the indicators of the control group with negative ammonia expression. In the cortex this relation was 72.15 (69.32; 77.45) vs. 18.14 (15.26; 19.53) CUOD (297.73% higher); thalamus – 112.04 (106.74; 115.25) vs 19.25 (16.58; 19.72) CUOD (482.02% higher); striatum – 103.46 (101.12; 107.29) vs 18.46 (15.69; 18.93) CUOD (460.45% higher); cerebellum – 118.45 (110.29; 121.62) vs 19.74 (18.32; 19.83) CUOD (500.00% higher), respectively (Fig. 1, 2). These data confirm the widely accepted hypothesis that implicates ammonia as a major neuroaggressive factor and trigger for HE development during liver failure [12, 13].



ACUOD – ammonia level (expressed in CUOD); AA2, n – Alzheimer 2 astrocytes (numbers); GFAP, S rel, % – relative area of GFAP immunopositivity; GS, S rel, % – relative area of GS immunopositivity; AQP4, S rel, % – relative area of AQP4 immunopositivity; CD68, S rel, % – relative area of CD68 immunopositivity; % CD68 ameb – the percentage of CD68<sup>+</sup> amoeboid microglial cells; % CASP3<sup>+</sup> neurons – the percentage of CASP3<sup>+</sup> neurons; Syn, CUOD – synaptophysin level expressed in CUOD; PVS+PCS, μm<sup>2</sup> – the average area of the extended tissue perivascular and pericyellular spaces expressed in μm<sup>2</sup>; AB, n – amyloid bodies (numbers).

**Fig. 1. Median indicators of pathomorphological parameters of the cerebral cortex (A), thalamus (B), striatum (C), and cerebellum (D) of deceased cirrhotic patients with HE Grade 3-4 during ACLF compared to control group**

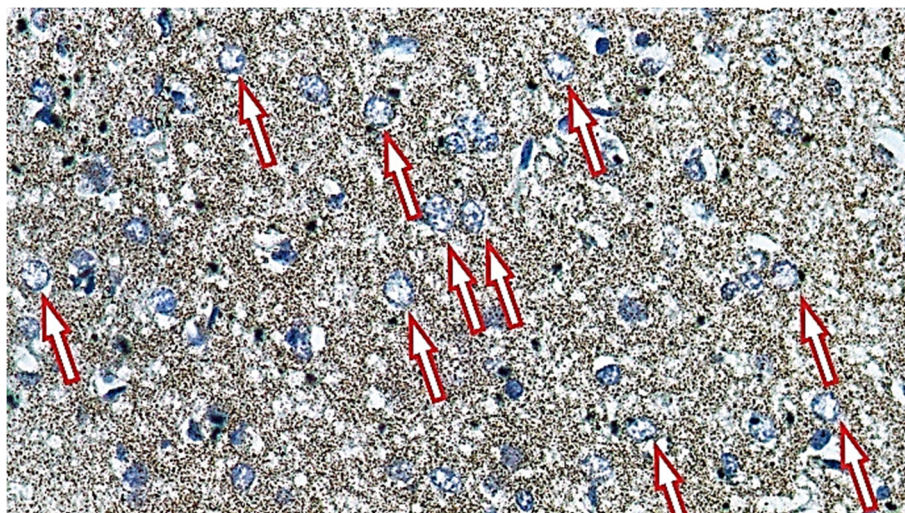


**Fig. 2. Strong («+++») brownish-colored histochemical expression (in CUOD) of the ammonia in tissue precipitates accompanied by the presence of numerous AA2-astrocytes (red arrows) in the thalamus of a deceased cirrhotic patient with HE Grade 4 (hepatic coma) during ACLF. HC reaction with Nessler's reagent. Mg. x 400**

According to our data, high amounts of tissue ammonia precipitates in HE during ACLF adversely affect neurons and synaptic transmission in the brain associating with a compound morpho-functional remodeling of the glioneuronal complex. In deceased cirrhotic patients with severe HE, there was a reliable ( $p < 0.05$ ) increase in the percentage of Caspase 3+ neurons in apoptotic state (compared to control): in the cortex, the relation was 13.02 (11.37; 14.56) vs 5.63 (3.29; 8.68)% (131.26% higher); thalamus – 10.26 (7.45; 12.04) vs 3.25 (2.74; 4.67)% (215.69% higher); striatum – 10.48 (7.46; 11.72) vs 4.37 (3.19; 5.72)% (139.81% higher); cerebellum – 9.26 (7.48; 10.36) vs 4.25 (2.16; 5.24)% (117.88% higher), respectively (Fig. 1). According to [1], in liver failure, apoptosis and selective cytolysis are characteristic morphological forms of neuronal death. P.R. Angelova et al. (2022) have evidenced that neuronal death during hepatic hyperammonemia is mostly conditioned by mitochondrial dysfunction mechanisms [14]. At the same time, signs of reduced neuronal synaptic transmission were registered in the brains of patients with severe HE in ACLF. Thus, synaptophysin expression reliably ( $p < 0.05$ ) reduced compared to control: in the cortex – 32.45 (30.97; 35.51) vs 61.65 (56.23; 71.34) CUOD (reduced by 89.98%); thalamus – 27.54 (25.68; 34.56) vs 60.48 (57.92; 65.35) CUOD (lower by 119.60%); striatum – 29.67 (27.51; 38.48) vs 54.72 (51.12; 58.63) CUOD (reduced by 84.42%); cerebellum – 37.64 (32.54; 41.83) vs 51.37 (48.63; 53.92) CUOD (lower by 36.47%), respectively (Fig. 1, 3). Decreased synaptic transmission in all studied brain regions can be explained by direct ammonia-induced severe neuronal dysfunction and more important widespread astroglial insufficiency; the latter, according to [15, 16], deter-

mines the dysfunction of perisynaptic astrocytic processes and disruption of synapses. A central role in this primary synaptic dysfunction may be played by ammonia-induced deficiency of membrane glutamate and glutamine transporters in astrocytes and neurons, leading to accumulation of glutamate in synaptic clefts and increased glutamine levels within astrocytes, leading to excitotoxic neuronal death and degenerative cytotoxic/osmotic swelling of astrocytes [12, 13].

In the brains of deceased patients with HE Grade 3-4, simultaneously with increased tissue ammonia, it was determined reliably ( $p < 0.05$ ) elevated compared to control IHC expression of GS – the main astrocyte-specific enzyme for ammonia detoxification. Median values of Srel.% of GS+ IPM were equal to: in the cortex – 16.27 (14.31; 18.43) vs 4.29 (2.26; 5.63)% (209.32% higher); thalamus – 7.59 (5.75; 9.51) vs 2.15 (1.73; 3.45)% (253.02% higher); striatum – 5.37 (5.18; 6.53) vs 1.84 (1.33; 2.12)% (191.84% higher); cerebellum – 7.32 (6.56; 9.25) vs 2.43 (0.63; 2.84)% (201.23% higher) respectively (Fig. 1, 4). Physiologically, astrocytes are the main brain cells responsible for the conversion of ammonia and glutamate to glutamine through catalysis by GS. Besides supposed dysfunction of SNAT-transporters removing glutamine from astrocytes to nearby neurons during HE [3], our study revealed that accumulation of glutamine osmolyte in astrocytes may also be due to an increase in its synthesis conditioned by increased GS expression. Such hyperexpression of GS is supposed to be a compensatory astrocytic response to accumulation of tissue ammonia and is consistent with reported experimental data on acute and chronic liver failure [17]. However, glutamine accumulation in these conditions is one of the most

detrimental for astrocytes and brain tissue as it leads to osmotic cellular edema. Moreover, glutamine (according to «Trojan Horse» hypothesis) can act as a Trojan Horse being a hidden ammonia carrier. Thus, being transported to the mitochondria via the glutamine transporter (GLN-Tx), glutamine undergoes

metabolism by phosphate-activated glutaminase into glutamate and ammonia. Accumulation of the latter instigate mitochondrial dysfunction, generation of reactive oxygen species, and tissue energy failure [16].

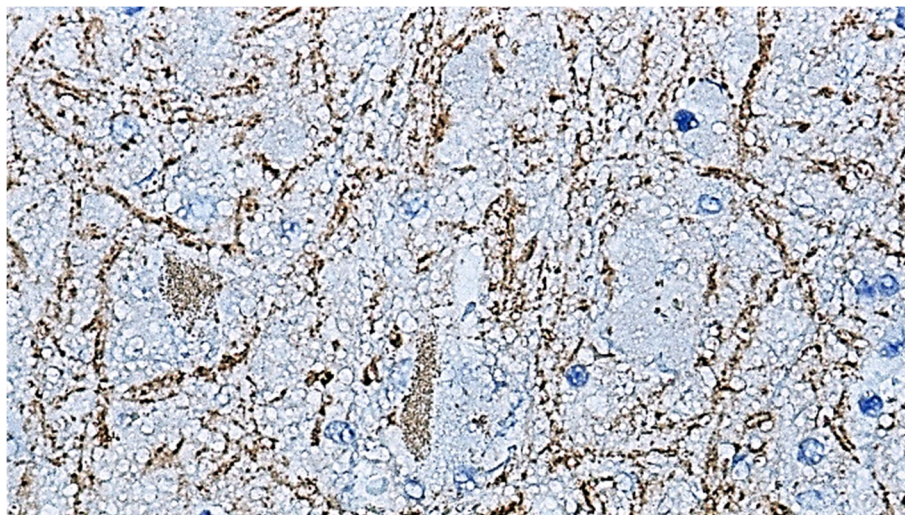


**Fig. 3. Weak synaptophysin expression (in CUOD) in the presynaptic membranes of interneuronal synapses of thalamus in the deceased cirrhotic patient with HE Grade 4 (hepatic coma) during ACLF. Mo monoclonal anti-synaptophysin Ab (Clone SY38, Thermo Scientific Inc., USA) Mg. x 400**

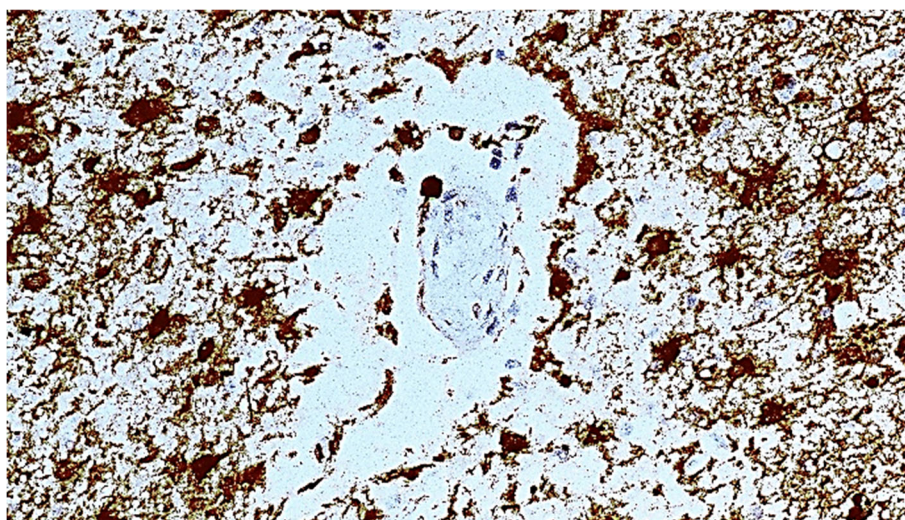


**Fig. 4. Extended area of GS expression in the thalamus of a deceased cirrhotic patient with HE Grade 4 (hepatic coma) during ACLF. Rb polyclonal anti-GS Ab (Thermo Scientific Inc., USA). Mg. x 400**

In all studied brain regions of deceased patients with ACLF and severe HE was observed a reliably ( $p < 0.05$ ) larger (compared to control) mean area of perivascular and pericellular «swollen» tissue spaces (PVs+PCs) which, according to electron microscopy, represent expanded perivascular and pericellular astrocytic processes [18]. Srel.% medians of these «swollen» tissue spaces were equal to: in the cortex – 102.64 (81.69; 105.68) vs 11.63 (9.48; 14.25)  $\mu\text{m}^2$  (782.54% higher); thalamus – 97.42 (85.12; 102.45)

vs 10.06 (8.15; 11.45)  $\mu\text{m}^2$  (868.38% higher); striatum – 93.55 (81.36; 99.39) vs 9.54 (9.32; 12.51)  $\mu\text{m}^2$  (880.60% higher); cerebellum – 101.36 (98.43; 110.15) vs 10.23 (9.98; 11.56)  $\mu\text{m}^2$  (890.81% higher), respectively (Fig. 1). At the same time, a reliably ( $p < 0.05$ ) higher compared control expression of the main brain water channel protein AQP4 was also determined. Srel.% indicators of AQP4+ IPM were: in the cortex – 15.64 (12.63; 17.12) vs 3.40 (3.22; 4.25)% (360.00% higher); thalamus – 8.32 (7.57; 9.37) vs

1.43 (0.43; 1.68)% (481.81% higher); striatum – 8.17 (6.86; 8.59) vs 1.95 (1.65; 2.43)% (318.97% higher); cerebellum – 9.75 (8.84; 11.93) vs 3.16 (2.47; 3.75)% (208.54% higher), respectively (Fig. 1, 5). The enlarged swollen tissue spaces in HE confirms the development of complex edematous mechanism presumably including both cytotoxic and vasogenic pathways. The first one was more evidenced for severe forms of HE type «A» during acute liver failure, while the second is more characteristic for persistent milder HE forms [1]. In both variants,

edematous spaces are predominantly reflect enlarged swollen astrocytes and their processes, which are the central to HE pathomorphology. AQP4, which is a universal actor in the water exchange mechanisms, when increased, also speaks in favor of both edematous pathways. This corresponds to the reports of experimental studies which established that hyperammonemic medium induces dysfunction of the blood-brain barrier (BBB), promotes hyperexpression of AQP4 and supports brain edema [3, 18].

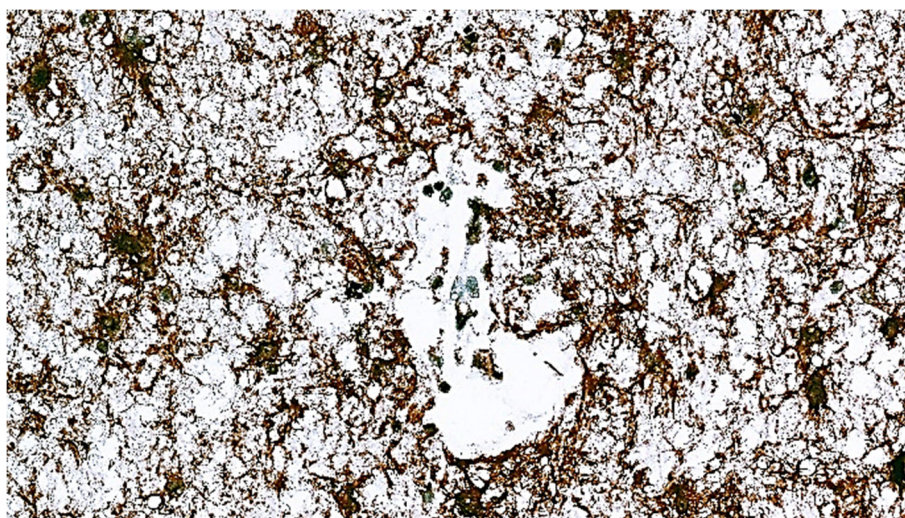


**Fig. 5. Extended area of AQP4 expression in the thalamus of a deceased cirrhotic patient with HE Grade 4 (hepatic coma) during ACLF. Rb polyclonal anti-AQP4 Ab (Thermo Scientific Inc., USA). Mg. x 400**

In deceased patients with ACLF and HE Grade 3-4, a significant ( $p < 0.05$ ) compared to control accumulation of amyloid bodies (AB) in the brain perivascular and subpial regions was determined. The median values of AB numbers were equal to: in the cortex – 5.00 (4.00; 6.00) vs 1.00 (0.00; 2.00) units (5-fold higher); thalamus – 7.00 (6.00; 9.00) vs. 2.00 (1.00; 3.00) units (3.5-fold higher); striatum – 6.00 (5.50; 8.00) vs 2.50 (1.00; 4.00) units (2.4-fold higher); cerebellum – 7.00 (6.50; 10.00) vs 2.00 (1.50; 2.00) units (3.5-fold higher) respectively (Fig. 1). There is growing body of evidence that AB are initially formed in astrocytic cytoplasm during utilizing their own and tissue decay products and gradually accumulate there like containers which subsequently released from astrocytes, migrate to the glymphatic system and transported to deep cervical lymph nodes, where they are eventually phagocytosed by local macrophages [19, 20]. It can be assumed that the accumulation of AB in severe HE may indicate the processes of active neutralization by astrocytes of the products of neurotoxin-induced disturbed metabolism and be a marker of partial

failure of the glymphatics, which cannot ensure timely transport of AB to the extracranial lymphatic system. Therefore, AB can be considered a putative marker of astroglial and glymphatic failure, which can be used to assess the functionality of the astrocytic syncytium in various neuropathologies.

Alzheimer type 2 astrocytes, widely considered the hallmark of HE, represent the morphological manifestation of profound dysmetabolic astrocytostrophy [21]. AA2 were extremely rarely observed in the brains of control patients, while in patients with ACLF and HE Grade 3-4 they were determined in reliably ( $p < 0.05$ ) higher numbers – median values of AA2 were equal to: in the cortex – 25.00 (21.50; 26.00) vs 3.00 (2.00; 4.00) units (8.33-fold higher); thalamus – 37.00 (22.50; 56.00) vs. 4.00 (3.00; 6.00) units (9.25-fold higher); striatum - 27.00 (24.50; 47.00) vs 3.00 (3.00; 5.00) units (9-fold higher); cerebellum – 33.00 (28.00; 54.00) vs 3.00 (4.00; 6.00) units (11-fold higher) respectively (Fig. 1, 2). Microscopically, AA2 have an enlarged watery nucleus with a scant marginal chromatin, excentric nucleolus, and thin rim of cytoplasm [4]. This astrocytic

morphotype is considered irreversible, followed by further vacuolar degeneration of the nucleus, endoplasmic reticulum, Golgi complex, and cell death [4]. Widespread appearing of AA2 in all studied brain regions confirms the value of these cells for diagnosis of severe HE. In support of the astrodystrophic concept, in deceased patients with ACLF and HE Grade 3-4, a significantly reduced (compared to control) Srel.% of intermediate filament protein GFAP+ IPM was revealed in astrocytes of all studied brain regions; the median values of which were: in the cortex – 1.24 (0.42; 1.38) vs 4.52 (4.23; 5.57)% (264.51% lower); thalamus – 1.74 (1.06; 1.86) vs 6.36 (5.91; 6.79)% (265.51% lower); striatum – 1.57

(1.05; 1.77) vs 6.23 (5.70; 7.84)% (296.81% lower); cerebellum – 1.88 (1.75; 2.03) vs 5.59 (5.18; 5.83)% (197.34% lower), respectively ( $p < 0.05$ ) (Fig. 1, 6). Although neuroinflammatory mechanisms is considered to play an important role in the development of HE, and increased GFAP levels have been suggested (as is typically seen during astrocyte reactivity in an inflammatory environment), we found the opposite response. According to [1, 18], revealed decreased GFAP expression confirmed the loss of control by astrocytes over synthesis of their cytoskeletal proteins in a hyperammonemic media contributing to their transformation into AA2.

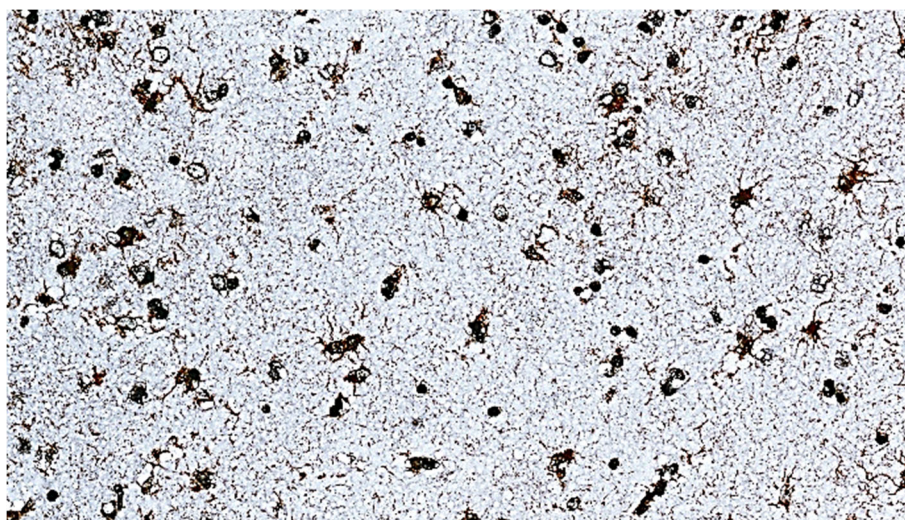


**Fig. 6. Decreased GFAP expression in the cerebral cortex of a deceased cirrhotic patient with HE Grade 4 (hepatic coma) during ACLF. Mo monoclonal anti-GFAP Ab (clone ASTRO6, Thermo Scientific Inc., USA). Mg. x 200**

It is believed that in HE there is no remarkable BBB disruption for proteins and cells, therefore the number of hematogenous immunocompetent cells/macrophages in the brain tissue does not increase significantly [18]. Similarly to control group, in the brains of deceased patients with ACLF and HE Grade 3-4, most of the extravascular CD68+ cells had the morphology of surveilling microglia: a small body and elongated dichotomously branched processes; a small percentage of CD68+ amoeboid microglia was also observed. However, compared to control, Srel.% of extravascular CD68+ microglia in patients with ACLF and HE Grade 3-4 was significantly ( $p < 0.05$ ) higher; the median values were: in the cortex – 7.41 (6.56; 7.83) vs 3.45 (2.37; 4.68)% (114.78% higher); thalamus – 5.69 (4.47; 6.14) vs 3.63 (2.12; 3.97)% (56.74% higher); striatum – 5.47 (4.86; 5.89) vs 3.21 (2.67; 4.14)% (70.40% higher); cerebellum – 6.37 (5.59; 6.85) vs 3.25 (2.44; 4.34)% (96.00% higher), respectively. The percentage of

CD68+ amoeboid microglia was also reliably ( $p < 0.05$ ) increased compared to control indicators: in the cortex – 6.12 (4.45; 7.24) vs 3.56 (3.14; 4.26)% (71.91% higher); thalamus – 4.50 (4.15; 9.42) vs 2.72 (2.54; 3.69)% (65.44% higher); striatum – 4.25 (4.12; 7.86) vs 3.26 (2.46; 4.07)% (30.36% higher); cerebellum – 6.23 (5.68; 11.45) vs 4.36 (3.64; 4.83)% (42.88% higher) respectively (Fig. 1, 7). Neuroinflammatory component of HE pathophysiology was proven decades ago when microglial reactive response was shown central to propagation of detrimental cytokin cascades predominantly involving neuroglial cells [17]. Reactive microglial changes during persistent HE, associate with both phagocytic cleansing function and detrimental cytotoxic effects on astrocytes, neurons, and oligodendrocytes. In this study we have established that severe HE Grade 3-4 during ACLF (accompanied by serious systemic inflammation) is characterized by increased number of activated microglia, however, with a small proportion



of microgliaocytes involved in phagocytosis. Similar results were obtained by I. Zemtsova et al. [22] in the postmortem material of cirrhotic patients with HE and in the models of chronic and acute hyperammonemia *in vivo*: they showed ammonia-activated microglia with increased Iba-1 expression, 65% of which

showed reduced phagocytosis of latex particles. This phenomenon can supposedly be explained by the suppressive effect of high concentrations of tissue ammonia on the synthesis of microglial proteins responsible for the processes of phagocytosis.

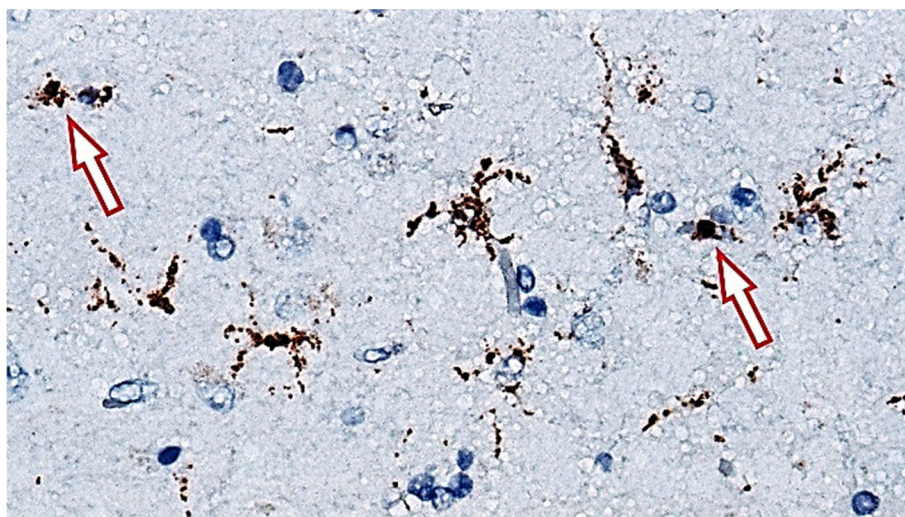


**Fig. 7. CD68 expression mainly in surveillant microglia and only single amoeboid microgliaocytes (red arrows) present in the cortex of a deceased cirrhotic patient with HE Grade 4 (hepatic coma) during ACLF. Mo monoclonal a-Hu CD68 Ab (clone PG-M1, RTU, Dako, Denmark) Mg. x 400**

#### CONCLUSION

Cerebral cortex, thalamus, striatum, and cerebellum of the deceased patients with severe hepatic encephalopathy Grade 3-4 as a component of acute-on-chronic liver failure (compared to control deceased patients) are characterized by: 1) histochemically determined moderate and strong granular expression of tissue ammonia; 2) increased numbers of apoptotic neurons (by caspase-3 expression); 3) decreased expression of synaptophysin in interneuronal synapses; 4) increased expression of astrocytic aquaporin-4; 5) significantly enlarged area of «swollen» perivascular and pericellular spaces; 6) significant accumulation of amyloid bodies; 7) increased expression of astrocytic glutamine synthetase; 8) reduced expression of glial fibrillary acidic protein in astrocytes; 9) pronounced Alzheimer type 2-astrocytosis; 10) moderate increase in cluster differentiation-68<sup>+</sup> microglia immunoreactivity accompanied by a small percentage of cluster differentiation-68<sup>+</sup> amoeboid microgliaocytes.

#### Contributors:

Shulyatnikova T.V. – conceptualization, methodology, resources, investigation, formal analysis, validation, visualization, writing – original draft;

Tumanskiy V.O. – conceptualization, methodology, supervision, project administration, writing – review & editing;

Tumanska L.M. – conceptualization, methodology, writing – review & editing.

**Funding.** This study was conducted in the framework of the scientific research work of Zaporizhzhia State Medical University “The morphogenesis of destructive-reparative processes of the brain in the diseases of vascular and toxic-metabolic origin”, number of state registration 0118U004253 (2018-2022) of the Ministry of Health of Ukraine.

**Conflict of interests.** The authors declare no conflict of interest.

#### REFERENCES

1. Butterworth RF. Hepatic Encephalopathy in Cirrhosis: Pathology and Pathophysiology. *Drugs*. 2019 Feb;79(Suppl 1):17-21.  
doi: <https://doi.org/10.1007/s40265-018-1017-0>

2. Görg B, Karababa A, Häussinger D. Hepatic Encephalopathy and Astrocyte Senescence. *J Clin Exp Hepatol*. 2018 Sep;8(3):294-300.  
doi: <https://doi.org/10.1016/j.jceh.2018.05.003>

3. Elsherbini DMA, Ghoneim FM, El-Mancy EM, Ebrahim HA, El-Sherbiny M, El-Shafey M, et al. Astrocytes profiling in acute hepatic encephalopathy: Possible enrolling of glial fibrillary acidic protein, tumor necrosis factor-alpha, inwardly rectifying potassium channel (Kir 4.1) and aquaporin-4 in rat cerebral cortex. *Front Cell Neurosci.* 2022 Aug 17;16:896172. doi: <https://doi.org/10.3389/fncel.2022.896172>
4. Shulyatnikova TV, Tumanskiy VO. Ammonia level and Alzheimer type 2 astrocytes in the brain of deceased patients with liver cirrhosis of the varying degree. *Pathologia.* 2023 Apr 28;20(1):36-44. doi: <https://doi.org/10.14739/2310-1237.2023.1.276453>
5. Arroyo V, Moreau R, Jalan R. Acute-on-Chronic Liver Failure. *N Engl J Med.* 2020 May 28;382(22):2137-45. doi: <https://doi.org/10.1056/NEJMra1914900>
6. Engelmann C, Berg T. Clinical practice guidelines for acute-on-chronic liver failure: are we ready for reaching global consensus? *Hepatobiliary Surg Nutr.* 2023 Apr 10;12(2):239-43. doi: <https://doi.org/10.21037/hbsn-23-6>
7. Zaccherini G, Weiss E, Moreau R. Acute-on-chronic liver failure: Definitions, pathophysiology and principles of treatment. *JHEP Rep.* 2020 Sep 2;3(1):100176. doi: <https://doi.org/10.1016/j.jhepr.2020.100176>
8. Nakadate K, Sono C, Mita H, Itakura Y, Kawakami K. Severe Acute Liver Dysfunction Induces Delayed Hepatocyte Swelling and Cytoplasmic Vacuolization, and Delayed Cortical Neuronal Cell Death. *Int J Mol Sci.* 2023 Apr 16;24(8):7351. doi: <https://doi.org/10.3390/ijms24087351>
9. Kok B, Abraldes JG. Child-Pugh Classification: Time to Abandon? *Semin Liver Dis.* 2019 Feb;39(1):96-103. doi: <https://doi.org/10.1055/s-0038-1676805>
10. Gutiérrez-de-Juan V, López de Davalillo S, Fernández-Ramos D, Barbier-Torres L, Zubiete-Franco I, Fernández-Tussy P, et al. A morphological method for ammonia detection in liver. *PLoS One.* 2017 Mar 20;12(3):e0173914. doi: <https://doi.org/10.1371/journal.pone.0173914>
11. Antomonov MYu. [Mathematical processing and analysis of medical and biological data. 2nd ed.]. Kyiv: "Medinform"; 2018. 579 p. Russian.
12. Lu K. Cellular Pathogenesis of Hepatic Encephalopathy: An Update. *Biomolecules.* 2023 Feb 19;13(2):396. doi: <https://doi.org/10.3390/biom13020396>
13. Jayakumar AR, Norenberg MD. Hyperammonemia in Hepatic Encephalopathy. *J Clin Exp Hepat.* 2018;8(3):272-80. doi: <https://doi.org/10.1016/j.jceh.2018.06.007>
14. Angelova PR, Kerbert AJC, Habtesion A, Hall A, Abramov AY, Jalan R. Hyperammonaemia induces mitochondrial dysfunction and neuronal cell death. *JHEP Rep.* 2022 May 23;4(8):100510. doi: <https://doi.org/10.1016/j.jhepr.2022.100510>
15. Popek M, Bobula B, Sowa J, Hess G, Polowy R, Filipkowski RK, et al. Cortical Synaptic Transmission and Plasticity in Acute Liver Failure Are Decreased by Presynaptic Events. *Mol Neurobiol.* 2018 Feb;55(2):1244-58. doi: <https://doi.org/10.1007/s12035-016-0367-4>
16. Häussinger D, Dhiman RK, Felipo V, Görg B, Jalan R, Kircheis G, et al. Hepatic encephalopathy. *Nat Rev Dis Primers.* 2022 Jun 23;8(1):43. doi: <https://doi.org/10.1038/s41572-022-00366-6>
17. Jaeger V, DeMorrow S, McMillin M. The Direct Contribution of Astrocytes and Microglia to the Pathogenesis of Hepatic Encephalopathy. *J Clin Transl Hepatol.* 2019 Dec 28;7(4):352-61. doi: <https://doi.org/10.14218/JCTH.2019.00025>
18. Claeys W, Van Hoecke L, Lefere S, Geerts A, Verhelst X, Van Vlierberghe H, et al. The neuroglivascular unit in hepatic encephalopathy. *JHEP Rep.* 2021 Aug 11;3(5):100352. doi: <https://doi.org/10.1016/j.jhepr.2021.100352>
19. Augé E, Bechmann I, Llor N, Vilaplana J, Krueger M, Pelegrí C. Corpora amylacea in human hippocampal brain tissue are intracellular bodies that exhibit a homogeneous distribution of neo-epitopes. *Sci Rep.* 2019 Feb 14;9(1):2063. doi: <https://doi.org/10.1038/s41598-018-38010-7>
20. Riba M, Augé E, Campo-Sabariz J, Moral-Anter D, Molina-Porcel L, Ximelis T, et al. Corpora amylacea act as containers that remove waste products from the brain. *Proc Natl Acad Sci USA.* 2019 Dec 17;116(51):26038-48. doi: <https://doi.org/10.1073/pnas.1913741116>
21. Agarwal AN, Mais DD. Sensitivity and Specificity of Alzheimer Type II Astrocytes in Hepatic Encephalopathy. *Arch Pathol Lab Med.* 2019 Oct;143(10):1256-8. doi: <https://doi.org/10.5858/arpa.2018-0455-OA>
22. Zemtsova I, Görg B, Keitel V, Bidmon HJ, Schrör K, Häussinger D. Microglia activation in hepatic encephalopathy in rats and humans. *Hepatology.* 2011 Jul;54(1):204-15. doi: <https://doi.org/10.1002/hep.24326>

Стаття надійшла до редакції 06.04.2024;  
затверджена до публікації 31.05.2024

